polymer papers

The application of mixed crystal i.r. spectroscopy to molecular deformation in polyethylene by rolling

Emmanuel U. Okoroafor* and Stephen J. Spells†
Materials Research Institute, Sheffield Hallam University, Pond Street, Sheffield S1 1WB, UK
(Received 9 November 1993)

The mixed crystal i.r. technique has been applied to polyethylene single crystal mats after rolling at room temperature to roll ratios up to 6.0. Reduction in the absorbance of the outer CD_2 bending components provides evidence of lamellar breakup. Model calculations indicate that the size of blocks which break away from the crystals is reduced to ~36 Å for a roll ratio of 6, while X-ray diffraction data show that crystallite reorientation occurs progressively with increasing roll ratio. Changes in small-angle X-ray scattering and the Raman longitudinal acoustic mode with rolling demonstrate that crystallite stacking periodicity is gradually lost and that crystal thickness remains unchanged.

(Keywords: i.r. technique; mixed crystal; polyethylene)

INTRODUCTION

The production of polymers with enhanced physical properties, such as high modulus fibres, has led to detailed investigations of the underlying morphologies. In several cases, polyethylene single crystals have been used as well characterized model starting materials for studies of deformation. Several models have been proposed for the types of molecular reorganization which occur in semi-crystalline polymers during deformation[1-5]. All these feature molecular chain movement within the crystalline phase during deformation, but experimental evidence to support a specific model is often limited by the absence of data providing molecular (as opposed to morphological) information. In addition, owing to the brittleness of single crystal mats, most studies have only been carried out at high temperatures of deformation. Direct thermal effects on the molecular conformation are important at these temperatures and the relevance of the initial molecular conformation becomes unclear.

Recently, the isotopic labelling technique has been used to establish the conformation of individual polymer molecules in solution-grown single crystals of polyethylene[6,7]. Both i.r. spectroscopy and neutron scattering were used to obtain a detailed statistical model. Both techniques are sensitive to the pathway of individual molecules, rather than to an averaged bulk property such as electron density. To a large extent, the two methods are complementary: neutron scattering intensity depends on crystal 'stem' (the molecular traverse of the crystal) correlations over a wide range of distances, whereas the i.r. technique is predominantly dependent on nearest neighbour interactions. Nevertheless, these interactions may extend over much larger distances, depending on the statistical arrangement of the labelled stems within the crystal lattice. Indeed, the combination of these two techniques provides little room for ambiguity in chain conformation.

The present work represents the first part of a combined i.r. and neutron scattering study of deformation in polyethylene single crystals: the neutron scattering results appear in an accompanying paper[8]. To utilize the established chain conformation in the as-grown crystals, it is necessary to deform the mats at a low temperature, as will be demonstrated. This severely limits the deformation methods which can be used. We make use here of rolling the mats at room temperature, to minimize thermal effects on chain conformation. The mixed crystal techniques have the potential of providing unique information relevant to the molecular reorganization occurring with deformation: the progressive disruption of groups of labelled stems with increasing roll ratio can be monitored, independently of crystallite orientation. This key feature, namely the possibility of separating the effects of crystal disruption and crystal orientation, makes the mixed crystal methods valuable in determining the molecular mechanisms of deformation. Furthermore, model calculations based on different schemes of crystallite breakup allow the changing size of crystallite blocks to be estimated from the i.r. spectra.

EXPERIMENTAL

Initial molecular conformation

The starting point for any molecular rearrangement is taken as the model[6,7], shown schematically in *Figure 1* for the chain conformation in crystals grown from dilute

*Current address: Department of Chemistry and Physics, Nottingham Trent University, Nottingham NG11 8NS, UK
†To whom correspondence should be addressed

0032-3861/94/21/4578-12

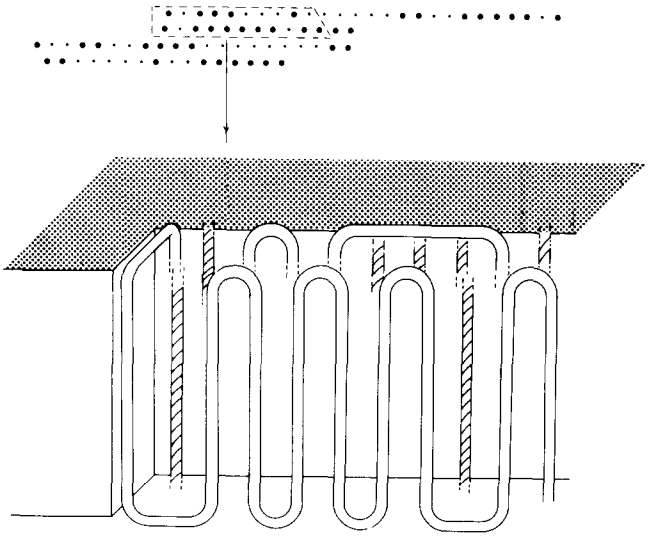

Figure 1 Schematic representation of the molecular conformation of a labelled polyethylene chain within the lamella. The large spots in the crystal stem projection at the top correspond to the unshaded molecule in the perspective sketch. The [110] direction is horizontal

xylene solution at 70°C. The full details of the model have been given in reference 7, and only the main features will be restated here. The crystal stems are arranged along sheets in the ⟨110⟩ directions. The stems do not show perfect adjacent re-entry: the fold plane is diluted with other molecules to the extent that 50% of the lattice sites along the ⟨110⟩ directions are occupied by stems from a labelled molecule. There is an occasional fold in a different direction, giving rise to another sheet of stems (four in the case of *Figure 1*). The number of sheets increases with guest molecular weight, with a molecular weight per sheet of 21 000. In fact, the only modification to the model on changing the label molecular weight is to change the number of sheets. The figure of 75% for the probability of adjacent re-entry produces small groups of adjacent stems along the fold plane. These were the main features of computer models which gave best agreement with i.r. bandshapes of the labelled molecules in the as-crystallized state: various arrangements of labelled crystal stems within a predominantly unlabelled lattice can give rise to splittings (the orthorhombic unit cell of crystalline polyethylene contains two symmetrically non-equivalent chains giving rise to both in-phase and out-of-phase modes in the i.r. spectrum of the labelled species). These splittings result primarily from interactions between labelled stems that are adjacent to one another in a ⟨110⟩ direction. The magnitude of the splitting is related to both the size and shape of a group of such adjacent labelled stems (on an orthorhombic lattice, there are four possible sites for nearest neighbours in ⟨110⟩ directions; if all these sites around a labelled stem are also occupied by labelled stems, the doublet splitting will be maximized) so that the conformation shown in projection at the top of *Figure 1* will produce several different doublet splittings. The isolated stems, together with amorphous chains, will give rise to a singlet peak.

If, during deformation, there is modification to the original arrangement of stems, due to crystalline lamellar breakup (accompanied by breaking up of the groups of adjacent labelled stems or by pull-out of stems), the original distribution of splittings would be modified to an extent dependent on the level of deformation. In fact, it is this important feature (the evolution of the distribution of splittings with deformation) that we utilize here in comparing i.r. experimental data with our model calculations simulating deformation of the crystalline lamellae.

I.r. spectrum calculation

The details of the technique, using the CX_2 bending vibration (X = H or D), have been described elsewhere[7,9], and only a brief outline will be given here. In the case of deformed polyethylene single crystals, the calculation of the guest species bending vibration lineshape follows along similar lines. First, the statistical model for the chain conformation in as-grown polyethylene single crystals is used to generate a set of molecular conformations (such as that shown in *Figure 1*). These arrangements of labelled stems are then divided into groups of stems in which there are ⟨110⟩ nearest neighbour interactions between all the labelled stems. A group transformation is then performed to obtain a simpler arrangement of stems for each group, but retaining the number of stems and distribution of nearest-neighbour interactions. The transformed group has been termed an 'equivalent group'[7]. The splitting of equivalent groups is then calculated using an interpolation based on calculated splittings for what were termed 'closed groups', i.e. groups with equal numbers of labelled stems in each sheet, all sheets starting in a single crystallographic plane and with no dilution of these planes by other molecule(s). The whole set of computer-generated molecular conformations is analysed in this way and the doublet components are summed, using empirical relationships established between the frequencies of both doublet components and the doublet splittings[9]. The doublet absorbances are weighted by the number of stems contributing to them.

A singlet component is included in the calculation. This includes contributions from labelled crystal stems that are isolated with regard to nearest neighbour labelled stems in the ⟨110⟩ directions and from non-crystalline chain segments. Crystallinity measurements by d.s.c. were used to calculate the singlet contribution from amorphous material. Finally, the calculated spectra were broadened by using a Lorentzian, with a bandwidth equal to the experimental resolution ($1.0\,cm^{-1}$).

Material preparation

Mixed crystals of normal polyethylene (PEH) and fully deuterated polyethylene (PED) were grown from dilute solution (0.05% w/v) of mixed xylenes at 70°C as described previously[10]. A PED concentration of 3% (in PEH) was used to ensure intramolecular interactions only among guest molecules. To observe the influence of molecular weight, two PED fractions of different molecular weights (*Table 1*) were co-crystallized separately with a PEH fraction ($\bar{M}_w = 86\,000$, $\bar{M}_n = 24\,000$). As the amounts of PED were too small to enable accurate molecular weight determination by g.p.c., the molecular weights shown in *Table 1* were estimated using neutron scattering and mixed crystal i.r. data since both techniques are sensitive to molecular weight, showing clear and reproducible trends in behaviour with changing molecular weight[6,7]. The assumption is made that the fractionation procedure has (as with previous samples) ensured polydispersities of $< \sim 1.4$.

Table 1 Samples used

Fraction	Molecular weight[a]	N_{sh}[b]
C	63000	3
A	150000	7

[a] Molecular weights estimated from both neutron scattering and mixed crystal i.r. spectroscopy
[b] Number of sheets used in molecular models

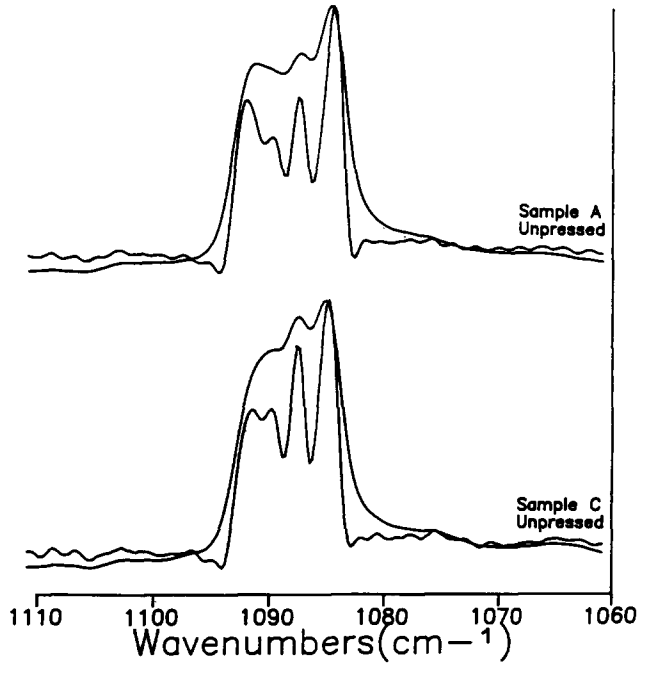

Figure 2 Evolution of the CD_2 bending vibration bandshape with molecular weight. Sample C, $M = 63000$; sample A, $M = 150000$. Raw and deconvoluted data are superimposed

The dried mixed crystal mats were then pressed at room temperature to minimize void scattering and afterwards deformed using the rolling technique. As the mats were very brittle (even after eliminating voids), and to achieve uniform deformation of the cut strips of mat at room temperature, the mats were first sandwiched between mild steel plates before being passed between rollers turning at a speed of 29 rev min^{-1}. Under these conditions, it was possible, at room temperature, to obtain samples with roll ratios, ε, in the range of 1 to 12. Some mats were pressed at higher temperatures, without rolling, to see if there would be any variation from the as-grown conformation with pressing temperature. Finally, since it has been observed that the as-grown conformation is modified in annealed polyethylene single crystals[11], we annealed some of our samples, to be able to compare the changes known to occur during annealing with those involved during mechanical deformation.

I.r. spectroscopy

A Mattson Galaxy 6021 Fourier transform i.r. spectrometer was used for the i.r. measurements using a mid-band MCT detector. Samples were mounted in a cell cooled to liquid nitrogen temperatures. A nominal resolution of 1.0 cm^{-1} was used, with 512 scans for each spectrum. As individual bandwidths within the CD_2 bending profile are $> 1.0\,cm^{-1}$, as are the separations between most of the components to be resolved, this resolution is adequate for the purposes here. Fourier self-deconvolution was used to improve the spectral resolution, with representative values of the deconvolution parameters σ (full width at half maximum absorbance for the intrinsic lineshape) and K (enhancement factor) of 2.5 cm^{-1} and 3, respectively. A Lorentzian lineshape was always used.

RESULTS

I.r. spectroscopy

In all spectra shown, the deconvoluted and raw spectra are superimposed. *Figure 2* shows the CD_2 bending vibration in the as-grown crystals for samples C and A. The absorbance and splitting ($\Delta\nu\,cm^{-1}$) of the outermost doublet increase with increasing PED molecular weight, while the absorbances of the inner doublets and the singlet decrease. This evolution of the bandshape with molecular weight is consistent with the model of the initial conformation for polyethylene single crystals shown in *Figure 1*: increasing molecular weight increases the number of superfolded sheets and consequently the size of adjacent ⟨110⟩ groups of stems also increases. The proportion of isolated stems and smaller groups of adjacent stems is thereby reduced, reducing the absorbance of the singlet and innermost doublets by comparison with the outermost doublets.

Figure 3 shows results for sample C after pressing (without rolling) at different temperatures, ranging from

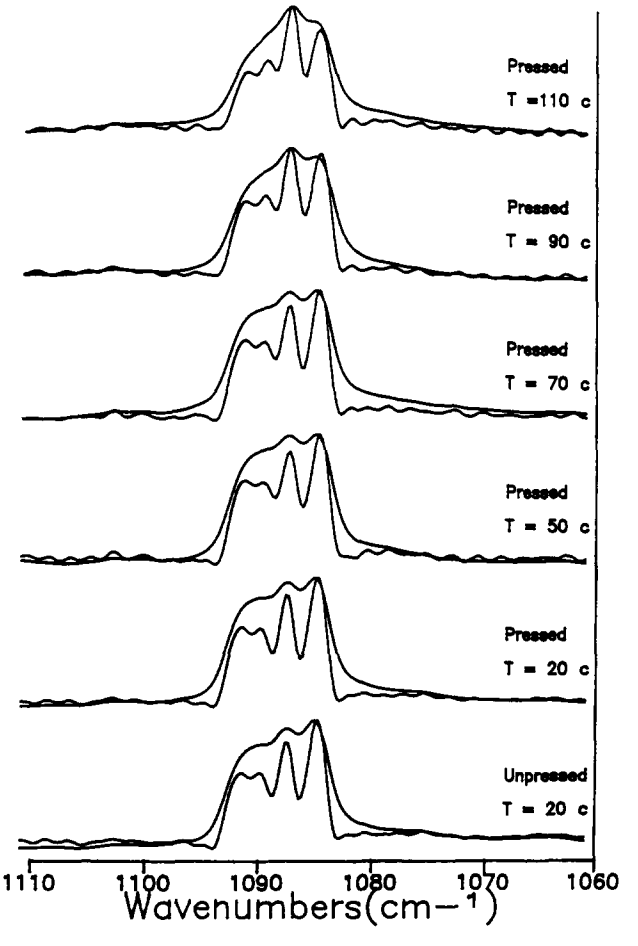

Figure 3 Variation of CD_2 bending vibration bandshape of sample C with press temperature. Raw and deconvoluted data are superimposed

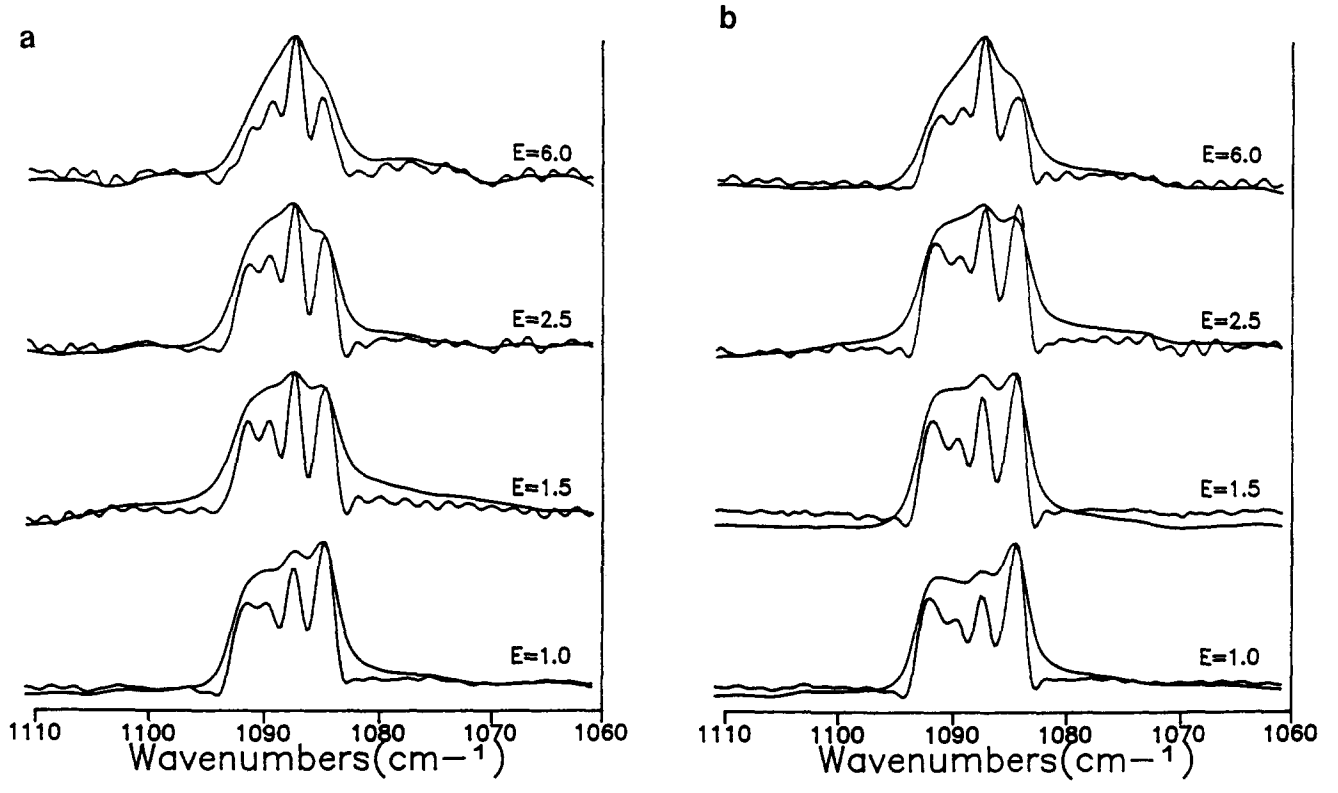

Figure 4 Variation of CD_2 bending vibration bandshape with roll ratio ε: (a) sample C ($M = 63\,000$); (b) sample A ($M = 150\,000$). Rolling was done at room temperature. Raw and deconvoluted data are superimposed

20 to 110°C (below the melting temperature of 132°C for crystals grown at 70°C). No significant change to the spectral bandshape occurs up to and including a press temperature of 70°C. However, at 90°C the bandshape is modified, notably with an increase in the singlet absorbance. Further increases in the press temperature increase the absorbances of the singlet and the innermost doublets with respect to the outermost doublet.

The same trend was observed with sample A. Note that the main reason for pressing the single crystal mats was to reduce void scattering without modifying the molecular conformation, orientation and texture in the as-grown crystals. From the figure, though, it is evident that molecular rearrangement is induced at high press temperatures, and this should be taken into account when samples are deformed at higher temperatures. This implies that, during deformation of single crystal mats at elevated temperatures ($80°C < T < T_m$), the mechanisms involved are not purely mechanical. Localized heating due to deformation could further raise the local temperature of the material, thereby allowing some molecular mobility. Indeed, the annealing behaviour of polyethylene is well-known and has previously been studied by the mixed crystal technique[11].

In order to observe the effects of mechanical deformation, without the complication of thermal effects, we present here results obtained with samples deformed at room temperature. *Figures 4a* and *b* show the i.r. spectra of samples C and A, respectively, deformed at room temperature to ε values ranging from 1.0 to 6.0. Both samples exhibited the same trend in the evolution of the spectral bandshape with ε; the absorbance of the outer doublets decreased with respect to those of the inner doublets and the singlet. In fact, at $\varepsilon = 6.0$ the singlet became predominant in both samples. At this ε, the outermost doublet is still present, although its absorbance has been reduced. These observations indicate that during deformation adjacent groups of stems break up, with the proportion of isolated stems and smaller groups of adjacent stems increasing at the expense of the larger groups of adjacent stems. The presence of the outermost doublet, up to $\varepsilon = 6.0$, is evidence that some of these larger groups are still retained. The latter implies that, at least for these rather low molecular weights, some of the features of the initial molecular conformation, such as the number of superfolded sheets, are still present up to $\varepsilon = 6.0$. Thus, either in the crystal blocks which have broken from the original lamellar crystals or in the remains of the original crystals themselves, there are still large groups of adjacent PED crystalline stems. Note also only minor changes in the spectrum up to $\varepsilon = 2.5$, indicating that the lamellar disruption initially proceeds slowly.

Figures 5a and *b* compare the spectra of the two samples (C and A) rolled to $\varepsilon = 6.0$ and the samples unrolled, but annealed at 120°C for 2 h. The spectral bandshape resulting from the thermal process, as for the mechanical process, showed an increase in the absorbance of the singlet and the inner doublets relative to the outer doublets. At this juncture, one is tempted to conclude that the same molecular mechanisms may be involved in both processes. However, a closer look at the spectra from the two processes reveals characteristic differences suggesting that the mechanisms involved might be different. The ratio of the absorbance of the lowest frequency component to that of the highest frequency component of the outermost doublet, remains unchanged on annealing the as-grown crystals. This ratio is considerably reduced on deformation, consistent with changes in orientation which are discussed below. More

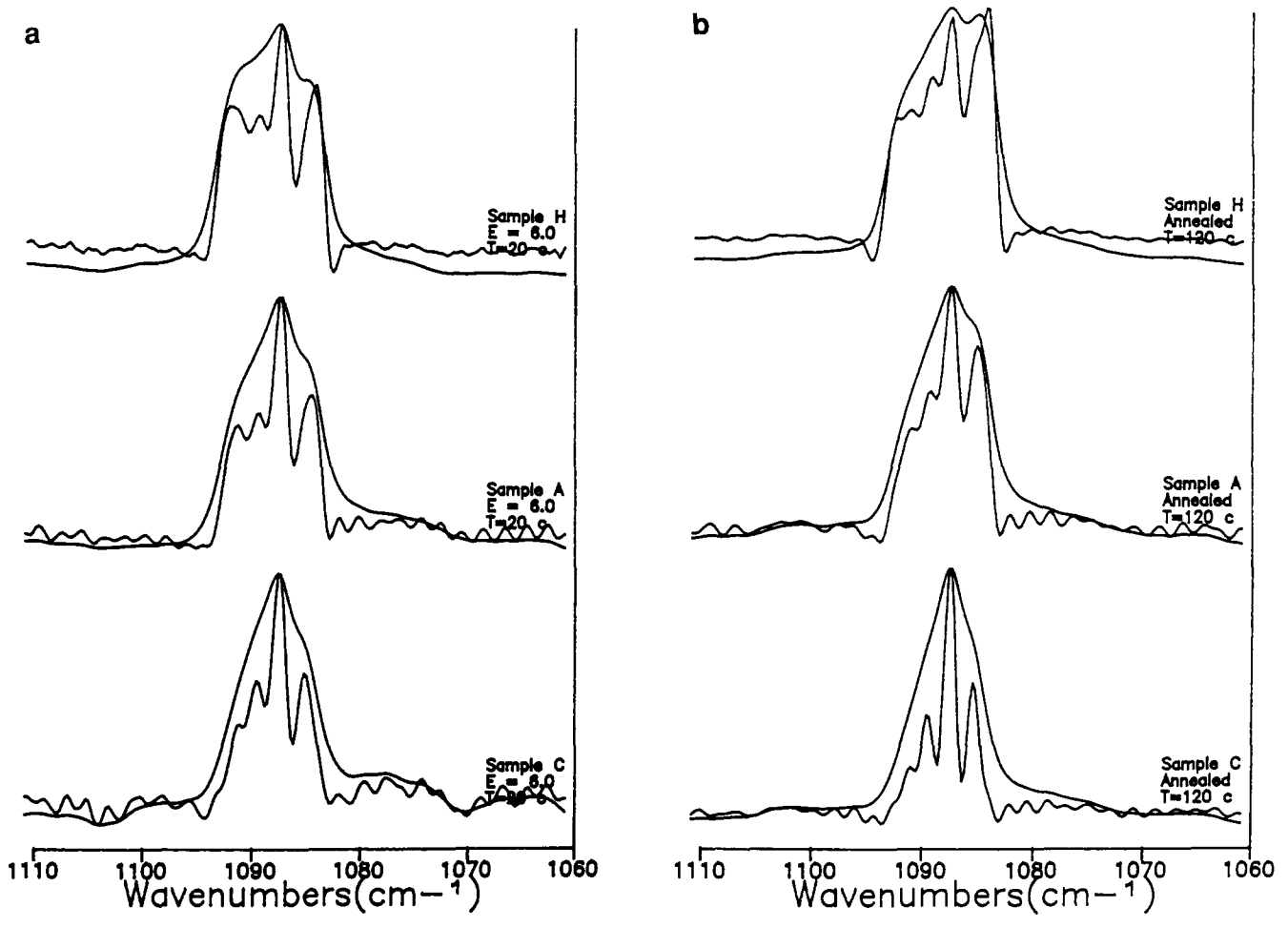

Figure 5 Comparison of spectral bandshape resulting from samples (a) rolled at room temperature to $\varepsilon = 6.0$ and (b) unrolled, but annealed at 120 C for 2 h. Raw and deconvoluted data are superimposed

importantly, it will be shown later that the long period of the mats does not change on rolling, whereas the changes in the i.r. spectrum on annealing are associated with the refolding necessary to accommodate the increase in long period[11].

We anticipate lamellar disintegration during rolling at room temperature, with the ensuing crystallites rotating so as to incline the molecular axis ultimately in the roll direction. Evidence for the type of orientation obtained has been collected from both polarized and unpolarized i.r. spectra. The dichroic ratio for both 1460 and 1474 cm^{-1} components of the CH_2 bending vibration was found to decrease with increasing ε, the change becoming smaller for $\varepsilon > 3.0$. The implication is that both *a*- and *b*-axes move away from the roll direction. Simultaneously, from unpolarized spectra, the 1460 cm^{-1} component decreases in absorbance with respect to the 1474 cm^{-1} peak and, for the CH_2 rocking vibration (*Figure 6*), the 733 cm^{-1} component decreases in absorbance with respect to the 721 cm^{-1} peak. For each of those vibrations, the absorbance of the *a*-polarized component is therefore reduced relative to that of the *b*-polarized component. This is attributable to the preferential alignment of the *b*-axis in the plane of the single crystal mat, while the *a*-axis leaves the plane and tends towards the normal to the mat plane. In these circumstances, one could only infer that the molecular axis (*c*-axis) tends towards the roll direction. In the same ε interval, the spectral bandshape of the PED bending vibration has also changed significantly, with the ratio of the absorbance for the low frequency component to that of the high frequency component of the doublets being reduced considerably. This change is not observed with annealed samples, and can only be associated with molecular reorientation due to rolling. On this evidence, molecular reorientation continues more slowly beyond $\varepsilon = 3$.

Figure 6 also includes evidence of the partial transformation of the orthorhombic structure of crystalline polyethylene into a monoclinic structure as demonstrated by the appearance of a characteristic absorption band at 717 cm^{-1}. The proportion of monoclinic phase in deformed samples of bulk crystallized polyethylene has previously been shown to depend in a complex way on the deformation history[12]. In our case, deconvolution of i.r. data revealed that, for ε values of 2 and above, the proportion of monoclinic material remained constant with increasing ε, suggesting a dynamic equilibrium between the two crystalline phases.

To summarize, the mixed crystal i.r. technique has provided information which seems to suggest that the initial molecular conformation (and hence the original lamellar crystals) breaks up during rolling and the crystallite blocks, detached from the lamellae, rotate so as to align the molecular axis (*c*-axis) in the roll direction. A more complete description of structural changes requires the consideration of possible refolding or changes in sample crystallinity with ε. For these, further information was sought using other techniques.

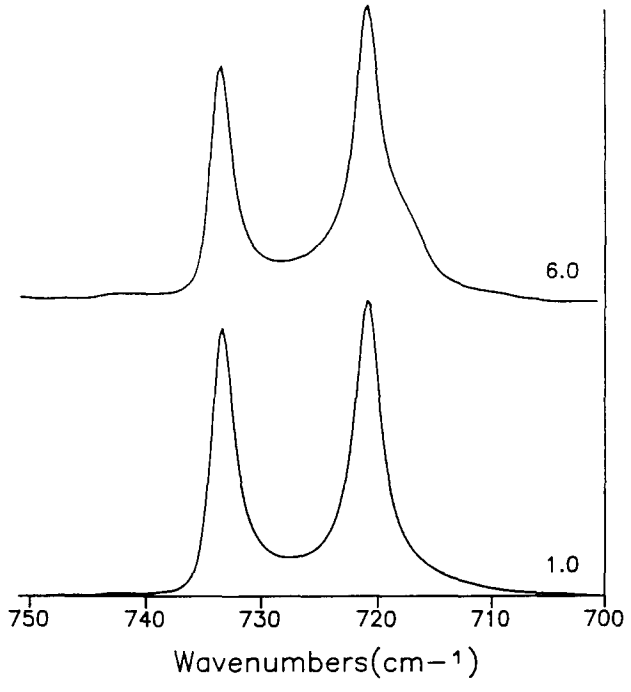

Figure 6 Changes in the CH_2 bending rocking vibrational bandshape with rolling. The ε values are indicated. The 733 cm^{-1} absorption band is associated with the crystallographic *a*-axis, and the 721 cm^{-1} band with the *b*-axis

Thermal analysis

The samples, both unrolled and rolled, were studied by d.s.c. A Mettler DSC 30 was used, with a heating rate of 10°C min^{-1}. The fusion peak temperature was shown to increase with increasing ε, accompanied by a reduction in crystallinity. Although the figures obtained for crystallinity may be influenced by effective constraints on the sample within the d.s.c. pan, the decrease in crystallinity nevertheless suggests a disruption of the original lamellar crystals, with some parts going into non-crystalline regions. As non-crystalline units also contribute to the i.r. absorbance of the singlet, the decrease in crystallinity could explain, in part, the considerable increase in the i.r. absorbance of the singlet.

Raman spectroscopy

Raman longitudinal acoustic mode (LAM) measurements were carried out on mats rolled at ambient temperatures to ε values up to 10.0, using a Spex triple monochromator spectrometer (1403/1442U) with spectral bandwidth 2 cm^{-1} and exciting wavelength 514 nm. The aim was to monitor the evolution of the crystal stem length with ε. The LAM profiles obtained and the calculated crystal stem lengths, based only on the LAM peak positions, are presented in *Figure 7*. Previous estimates of the combined constants[13] relating the LAM peak position to the stem length were used to calculate the crystal stem lengths here. The results indicate that the average stem length remained constant, while the scattered intensity decreased with increasing ε. This seems to suggest that an important fraction of the material with the initial stem length is maintained up to $\varepsilon = 10.0$, but that the initial structure has been disrupted. This result shows no clear indication of refolding to form thicker crystallites.

X-ray measurements

Small- and wide-angle X-ray scattering (SAXS and WAXS, respectively) measurements were also carried out on the same samples as were used for LAM measurements. The SAXS measurements were performed at the small-angle X-ray facility (station 8.2) at the Synchrotron Radiation Source (Daresbury), with radiation of wavelength 1.604 Å, using photographic film. Calibration was made using scattering from samples of rat-tail collagen. WAXS measurements were performed using a Worhus flat plate camera, with X-ray wavelength of 1.5 Å. Undeformed mats showed a long period of 110 Å and characteristic *c*-axis orientation.

SAXS results. *Figure 8* shows densitometer traces (radial scans) of the scattering obtained with increasing ε, where the X-ray beam is perpendicular to the roll direction and the mat normal. This indicates an unchanged periodicity up to $\varepsilon = 5.0$. The peak intensity decreased rapidly with ε, with no small angle peak observed beyond $\varepsilon = 5.0$. Rather, there was a considerable increase in the intensity of the diffuse scattering at very small angles. A uniform ring was obtained when $\varepsilon = 5.0$, indicating the change in crystallite orientation.

Clearly, the crystallite thickness does not change significantly with rolling. Coupled with the unchanging length of a chain traverse across the crystal, as determined from the Raman LAM data, this suggests that the tilt angle does not change to any great extent on rolling. The loss of intensity with increasing ε is probably caused by

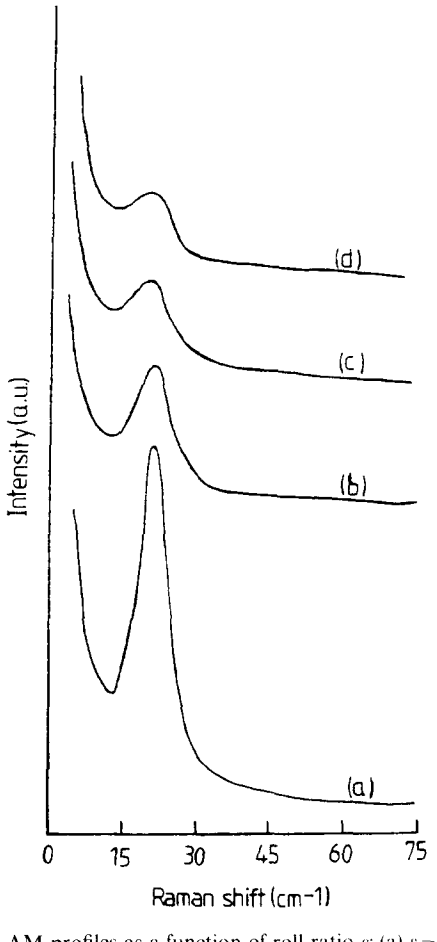

Figure 7 LAM profiles as a function of roll ratio ε: (a) $\varepsilon = 1.0$, crystal stem length (l_R) = 118 Å; (b) $\varepsilon = 2.5$, $l_R = 116$ Å; (c) $\varepsilon = 4.0$, $l_R = 121$ Å; (d) $\varepsilon = 10.0$, $l_R = 122$ Å

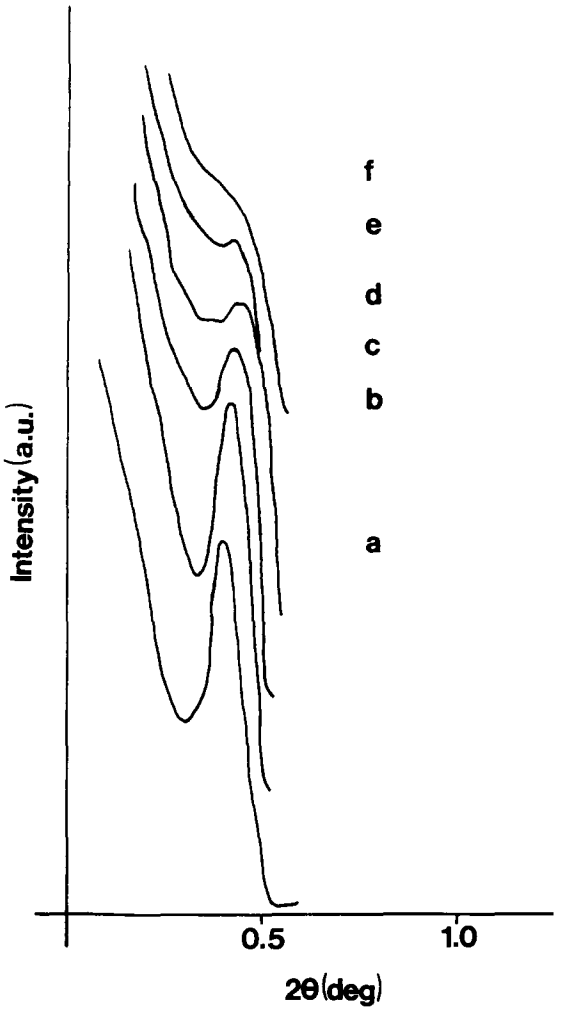

Figure 8 Densitometer traces (radial scan) of the SAXS patterns obtained for rolled polyethylene mats with the X-ray beam perpendicular to both the roll direction and the mat normal as a function of roll ratio ε. (a) $\varepsilon = 1.0$, long spacing (l_x) = 110 Å; (b) $\varepsilon = 1.5$, $l_x = 106$ Å; (c) $\varepsilon = 2.0$, $l_x = 106$ Å; (d) $\varepsilon = 2.5$, $l_x = 106$ Å; (e) $\varepsilon = 3.0$, $l_x = 106$ Å; (f) $\varepsilon = 5.0$, no peak in intensity

a lack of stacking regularity in the crystallites which have broken away from the original lamellae. Densification of the amorphous region by orientation and by chain segments pulled out of lamellar crystalline regions could also play a role. Crystallite translation and rotation, with the *c*-axis aligning with the roll direction, is consistent with these observations. This behaviour clearly differs from that observed for annealed single crystal mats rolled at elevated temperatures[14], where a four-point SAXS pattern develops from lamellar rotation and where it was suggested that the chain tilt angle approached a constant value.

WAXS analysis. Results from rolled samples showed clear parallels with earlier measurements on samples rolled after annealing[14]. The 200 reflections, initially equatorial for a sample with mat normal perpendicular to the X-ray beam, moved towards the meridian with increasing ε. However, the change in azimuthal intensity distribution with ε was significantly smaller in our case. The interpretation is that the *b*-axis tends towards a direction, within the mat plane, perpendicular to the roll direction, while the chain axis moves away from the mat normal.

In addition, the ratio of the intensities of the reflections 110 and 200 for the different arrangements gave information concerning the orientation of the crystallographic *a* and *b* axes in the deformed samples, the ratio became larger with increasing ε for the X-ray beam parallel to the mat normal and smaller for other scattering geometries. These features indicate that the unit cell *a*-axis is preferentially oriented perpendicular to the mat surface, and the *b*-axis parallel to the mat surface, with both axes perpendicular to the roll direction. This implies that crystallite rotation is preferentially about the crystallographic *b*-axis.

SUMMARY OF EXPERIMENTAL EVIDENCE

The mixed crystal i.r. technique applied to rolled samples of polyethylene single crystals has provided information on the breakup of crystalline lamellae during rolling, via the observation of breakup of groups of labelled crystal stems within the crystalline lamellae. The ensuing crystallites, whose average size depends on the level of deformation, retain some of the features of the initial molecular conformation and also tilt and rotate in the course of rolling, so as to align the molecular axis ultimately in the roll direction. It is interesting to note that the concept of crystalline blocks, the size of which changes, for example, on annealing, is not new: using the paracrystalline mosaic block model, Hosemann *et al.* obtained values in the region of 300–600 Å for annealed single crystals[15]. However, the blocks were envisaged as linked by twist grain boundaries, a highly specific model compared with ours.

In the present case, chain segments are believed to be pulled out from the crystallites in the course of translation and rotation as deformation proceeds, and there was no evidence of refolding. The other techniques employed to further elucidate the mechanisms involved during deformation of single crystals of polyethylene by rolling confirmed that the original lamellae are disrupted. The crystallites formed show changes in their size, perfection and surrounding environment with increasing ε. The crystal stem length within the crystallites remains the same as in the original lamellae. The crystallites preferentially rotate about their crystallographic *b*-axis, so as to align the molecular axis in the roll direction, with the *a*-axis tending towards the normal to the mat plane.

We now consider the i.r. data in more detail using the established molecular conformation in the as-grown crystals and computer models to represent several deformation processes which would affect the groupings of labelled stems.

MODELS OF MOLECULAR DEFORMATION

As mentioned earlier, the main features observed are lamellar disruption and subsequent reorientation of the ensuing crystallites during rolling. These molecular deformation mechanisms may be separated into two stages with increasing ε: (1) at the early stages of deformation, polyethylene single crystals crack up and tilt with the chain axis moving towards the roll direction. The crystallites are still large and the crack dimensions in the roll direction small and consequently there is little change in splittings. More cracks are generated with further tilting of the ensuing crystallites as deformation proceeds, but the crystallites so formed are generally of larger dimensions than individual labelled molecules; (2) the later stages of deformation are dominated by further

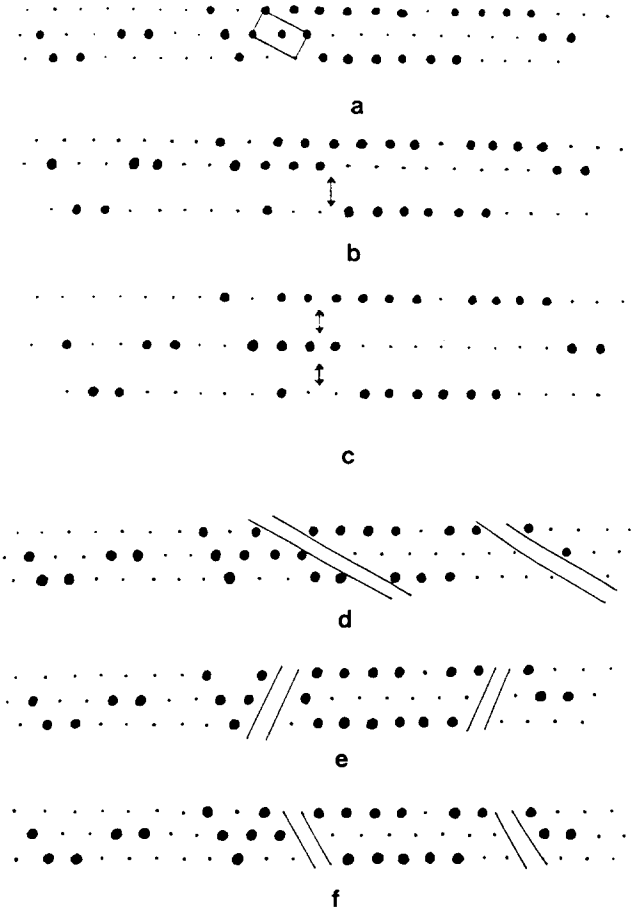

Figure 9 Schematic illustrations of the crack orientations during lamellar deformation: (a) undeformed; (b) partial sheet separation with cracks parallel to the fold direction; (c) total sheet separation; (d) cracks parallel to the crystallographic *a*-axis; (e) cracks parallel to the *b*-axis; (f) cracks parallel to non-folding ⟨110⟩ directions. The large dots represent the labelled crystal stem positions

breaks, intercrystallite separation and rotation about axes which are close to being perpendicular to the roll direction. The lateral size of crystallites formed now becomes smaller than labelled molecular dimensions, in addition to which the alignment towards the roll direction of chain segments pulled away from separating crystallites further reduces the size of the crystallites. This causes significant changes to the i.r. splittings. The original lamellar perfection and orientation is completely lost. It is, however, not implied here that there is any clear discontinuity in physical parameters of the type observed for single crystal mats annealed before rolling[14].

As pointed out earlier, the starting point for any molecular rearrangement will be taken as the established chain conformational model of polyethylene single crystals, shown schematically in *Figure 1*. However, in attempting to model the breakup of such an arrangement of labelled crystal stems, two main problems are encountered; namely the orientation of the cracks and the size distribution of the crystallites. Concerning crack orientation, it has been reported[16] that generally, during deformation, single crystals develop cracks in directions perpendicular to the axis of stretching, oriented along the planes (100), (010) and (110), and that the cracks may be empty or else penetrated by bundles of macromolecules, depending on the structure of the original crystal. Polyethylene single crystals demonstrate separate sectors (the number depending on the crystallization conditions, which in our case gave four domains) with different fold arrangements and orientation with respect to a given roll direction. Furthermore, the *c*-axis orientation of the original crystals ensures that the crystallographic *a*- and *b*-axes are randomly oriented in the mat plane. We shall therefore consider individually the influence on the labelled stem adjacency of cracks oriented along the aforementioned planes. Although deformation would inevitably result in a distribution of crystallite sizes, for simplicity we will subdivide the original arrangement into blocks of equal size (for a particular ε) and allow this size to decrease with increasing ε. This approach is essentially to reduce the number of computational parameters, since it is probable that cracks with different crystallographic orientations may occur simultaneously, together with some lamellae remaining undeformed.

Schematic diagrams, as shown in *Figures 9a–f* using an individual computer-generated molecular conformation (for a three-sheet model), will be employed to demonstrate the possible origins of the changes in the labelled stem adjacency during deformation of polyethylene single crystals. The figures correspond to a projection of the stem arrangement onto a {001} plane. The [110] fold direction coincides with the longer dimension of the figures, with the larger dots representing the labelled crystal stems. *Figure 9a* illustrates the as-grown undeformed molecule and includes the orthorhombic unit cell of crystalline polyethylene. The latter is essentially for the clarification of the crack orientation, with respect to the low index crystallographic directions within the original lamellar crystal.

Now we consider individually the influence on labelled stem adjacency of the cracks on a low index crystallographic direction. Each case will be considered as representative of the deformation mechanism of the entire material, with the cracks coinciding with the crystallographic direction under consideration, and oriented approximately at right angles to the roll direction.

Cracks parallel to the [110] fold direction

The cracks here would be oriented parallel to the (110) fold planes. This model would lead to what we term 'sheet separation' and the cracks would not be bridged by chain segments pulled from the separating sheets. These empty cracks could, however, be filled by other molecules as part of some co-operative process in the mat. *Figures 9b* and *c* show two cases corresponding, respectively, to partial and total sheet separation. In either case, such a process would generate smaller groups of labelled stems at the expense of the larger groups by reducing intersheet adjacency. Note, however, that this sheet separation process would maintain intrasheet labelled stem adjacency and dilution constant. This implies limited molecular continuity across the crack during the deformation process and is unlikely to explain the decrease in crystallinity observed for modest ε values. If total sheet separation is obtained with high ε values, then at such levels of deformation there would be no trace of the larger groups of labelled stems left. The outer i.r. doublets would then be lost at these high ε values, while the innermost doublets and the singlet would become predominant, indicating the disappearance of the superfolded molecular conformation. Should the separated sheets, or the blocks of crystal containing them, tilt or rotate so as to align the

molecular axis (*c*-axis) in the roll direction, then the *b*-axis while the *a*-axis inclines closer towards the mat plane. This would have the effect of diminishing the *b*-polarized absorbance relative to the *a*-polarized absorbance.

Slip in the chain direction has been widely discussed in terms of the deformation of polyethylene by drawing or rolling[2]. It should be noted that such slip may have a minor effect on the CD_2 bending lineshape, provided that the crystal stems remain adjacent for a sufficiently large number of repeat units ('fine slip'). The effects discussed in this section depend primarily on the separation of blocks, rather than slip itself.

Cracks parallel to the crystallographic a-*axis*

Figure 9d shows a schematic illustration of this process. The physical separation of neighbouring crystallite blocks during deformation interrupts the original groups of adjacent stems (as with all the other models here), reducing the CD_2 bending splittings. Here we rely on the fact that the interaction between labelled stems decreases rapidly with separation[17]. In the present case, due to chain topology ($\{110\}$ folding), there would be molecular continuity as the cracks would be bridged by chain segments pulled from adjacent crystal blocks (providing a possible explanation for the decrease in crystallinity with ε), and these segments would also contribute towards the absorbance of the singlet. The formation and separation of crystal blocks would clearly reduce the intrasheet labelled stem adjacency and dilution. The average crystallite size is expected to decrease with ε, either by the development of further cracks within existing crystallites or by chains unfolding as the crystal blocks rotate and separate (increasing crack dimensions) from each other. The formation of smaller groups of labelled stems obviously modifies the i.r. doublet splittings. However, unlike the 'sheet separation' model, the generation of smaller groups of labelled stems in this process, at the expense of the larger ones, appears to be a more gradual process: for sufficiently large block sizes, a multiple sheet-like structure would be maintained in the deformed samples, resulting in larger doublet splittings than for single sheets. If this were the case, then at high ε values one should still expect to see contributions from large groups of labelled stems to the i.r. spectrum. Here, crystal block rotation, so as to align the molecular axis in the roll direction, would incline the crystallographic *b*-axis towards the normal to the mat plane, while the *a*-axis remains in the plane of the mat. This molecular reorientation would reduce the *b*-polarized absorbance relative to the *a*-polarized absorbance.

Cracks parallel to the crystallographic b-*axis*

This model is presented schematically in *Figure 9e*. In fact, apart from the orientation of the cracks, this process should have similar effects to the preceding one with respect to the evolution of the labelled stem adjacency with increasing ε. Consequently, there should be a similar evolution of the absorbances of the singlet, inner doublets and outer doublets with ε. However, here crystal block rotation, to align the molecular axis in the roll direction, would incline the crystallographic *a*-axis towards the mat normal, while the *b*-axis remains in the plane of the mat, thereby reducing the *a*-polarized absorbance relative to the *b*-polarized absorbance.

Cracks parallel to non-folding $\langle 110 \rangle$ *directions*

This process, as shown schematically in *Figure 9f*, should, like the two preceding ones, present similar characteristics as to the evolution of the labelled stem adjacency and consequently the i.r. lineshape with ε. Crystal block rotation, in order to align the molecular axis in the roll direction would here incline the crystallographic *a*-axis closer towards the normal to the mat plane and the *b*-axis closer towards the plane of the mat, thereby reducing the *a*-polarized absorbance relative to the *b*-polarized absorbance.

We now present calculations based on these models and compare them with experimental results to determine which models provide a satisfactory fit to experimental data. Note that, as in previous work, a comparison between model calculations and deconvoluted experimental spectra provides a more rigorous test than if the raw data were used.

MODEL RESULTS

The model calculations are based on initial molecular conformations with three and seven sheets, which were found to be compatible with the molecular weights of samples C and A, and also showed good agreement with the experimental CD_2 bending vibration bandshape for corresponding as-crystallized samples. Following the model description, with cracks oriented with respect to specific crystallographic directions, the set of computer generated as-grown molecular conformations, involving ~ 5000 labelled stems, were broken up into blocks of equal size. We then have the problem of specifying the extent of rotation of the blocks broken from the original lamellar crystals. Although this could be approached statistically, we decided to introduce the average orientation experimentally determined from i.r. and WAXS into the model calculations. Finally, the i.r. spectrum was calculated as outlined above. Several crystal block sizes and crack dimensions (such that the ratio of the linear dimension occupied by the crystal block plus the separation in the deformed conformation to the linear dimension in the initial undeformed conformation is equal to the macroscopic ε) were tested to find the best fit to experimental bandshape with respect to ε. *Figure 4* shows the experimental data (including the ε values) and *Figures 10* and *11* the calculated results (including the crystal block sizes) for the deformation processes considered, starting with initial conformations with three and seven sheets, respectively.

Figures 4a and *b* show the experimentally observed evolution of the i.r. bandshape (raw and deconvoluted) with ε, for samples C ($\equiv 3$ sheets) and A ($\equiv 7$ sheets). The absorbances of the singlet and the inner doublets ($\Delta\nu = 4.5\,cm^{-1}$) increase relative to those of the outermost doublets ($\Delta\nu_C = 6.9\,cm^{-1}$; $\Delta\nu_A = 7.7\,cm^{-1}$). The ratio of the *a*-polarized absorbance (low frequency component) to the *b*-polarized absorbance (high frequency component) decreases with increasing ε, an indication of the preferred orientation of the crystallographic *b*-axis in the plane of the mat, relative to the *a*-axis, which tends towards the normal to the mat plane. Moreover, the presence of the outermost absorbance, even at $\varepsilon = 6.0$, indicates that the superfolded structure is not completely lost at such ε values. *Figures 10a* and *11a* show the calculated data for the sheet separation process. In fact, for such a process to be conceivable, we had to employ crystal block sizes

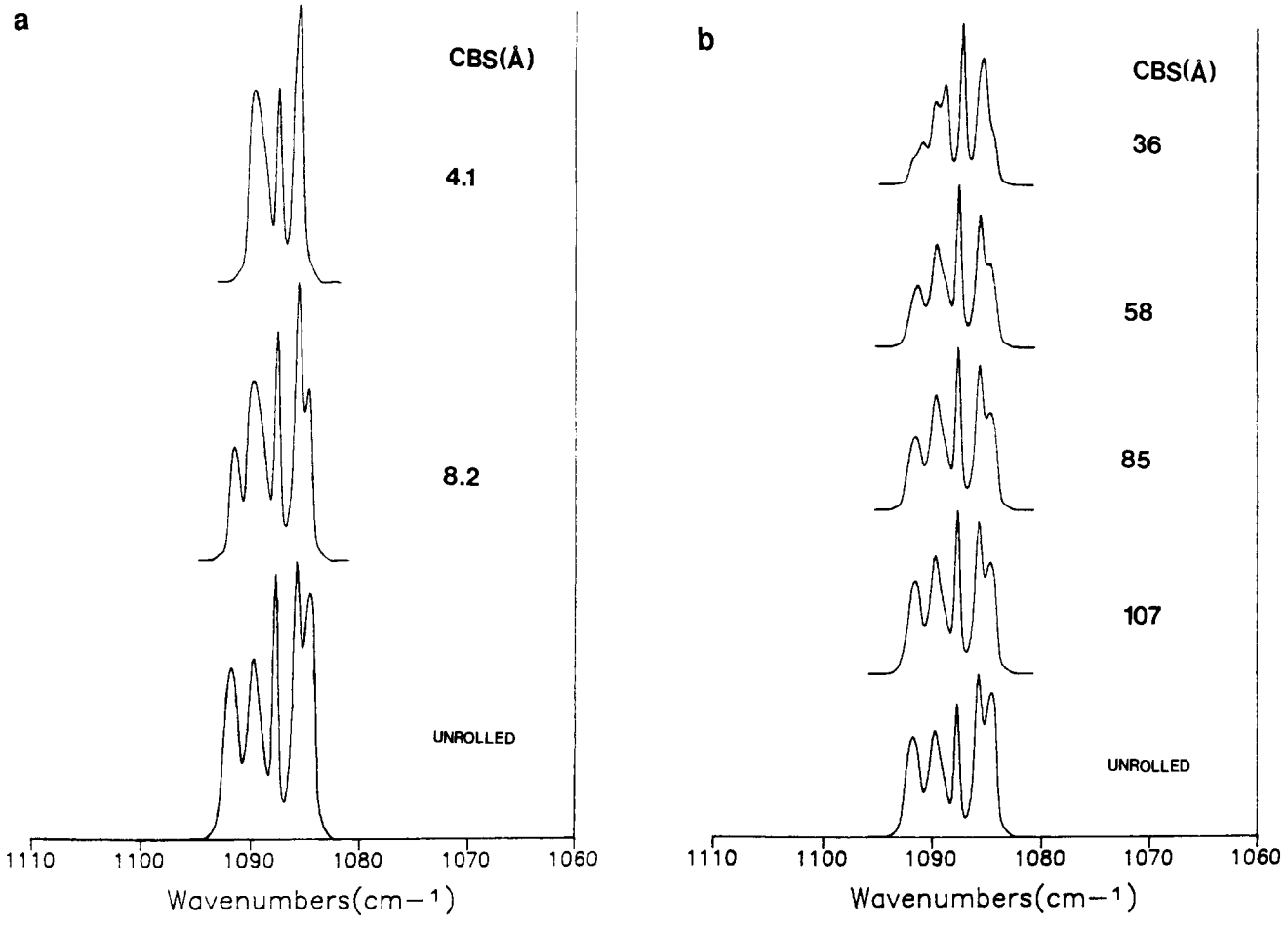

Figure 10 Calculated i.r. spectral bandshape for a three-sheet model as a function of crystal block size (CBS), for (a) the sheet separation process and (b) for cracks parallel to the crystallographic *a*-axis. For the sheet separation process, the cracks are parallel to the [110] fold direction

(as shown in the figures) of the order of the initial inter-sheet distances (4.11 Å). Evidently, this sheet separation model cannot be representative of the molecular deformation mechanisms of the crystalline lamellae—at least at modest ε values—since, even at total sheet separation, when the outermost splitting ($\Delta\nu_{3\text{sheets}} = 6.8\,\text{cm}^{-1}$; $\Delta\nu_{7\text{sheets}} = 7.9\,\text{cm}^{-1}$) had disappeared leaving only the innermost splitting ($\Delta\nu = 4.2\,\text{cm}^{-1}$), the singlet was still not predominant. This disagreement with experimental data is due mainly to the preservation of complete single sheets in the model, retaining the high intrasheet adjacency and low dilution of the original conformation. In addition, the larger groups of labelled stems rapidly decrease in size with this model. This does not entirely preclude the sheet separation process, but rather suggests that it is in no way representative of the deformation mechanism of crystalline lamellae, at least for modest ε values.

Figures 10b and *11b* show results obtained for the deformation process with cracks parallel to the crystallographic *a*-axis. These results are remarkably similar to calculations carried out for cracks parallel to the *b*-axis and for cracks parallel to non-folding ⟨110⟩ directions. The calculated spectra from the different processes show good agreement with experimental spectra for appropriate values of crystallite dimensions. Having chosen the value of crystal block size for a model calculation (using any of these three models) to best fit the experimental data for a particular ε, the relationship between crystal block size and ε shown in *Figure 12* was derived. It is significant that for these models, unlike in the 'sheet separation' process, the large groups do not rapidly decrease in size with increasing ε. The similar effects of the three different processes raise the possibility that the different mechanisms may be occurring together. In reality, energetic considerations might also play a role in determining the extent of this. If, however, they do occur together, then the relative frequency of the processes must be consistent with the observed preferential orientation of the crystallographic *b*-axis in the plane of the mat, with the *a*-axis tending towards the mat normal, as noted earlier. It is possible that an association of the processes could be attributed to the sectored structure of polyethylene single crystals, a feature which will be discussed below. Nevertheless, the main features emerging from this study are the estimates of crystallite block size over a range of ε values and the ability to correlate these figures with the changing crystal orientation (from X-ray diffraction).

DISCUSSION

The mixed crystal i.r. technique has provided direct evidence of the breakup of crystallites with rolling at room temperature under which conditions direct thermal effects are not relevant. A proportion of monoclinic phase is produced on rolling. Other techniques have been used to demonstrate the orientational changes which occur,

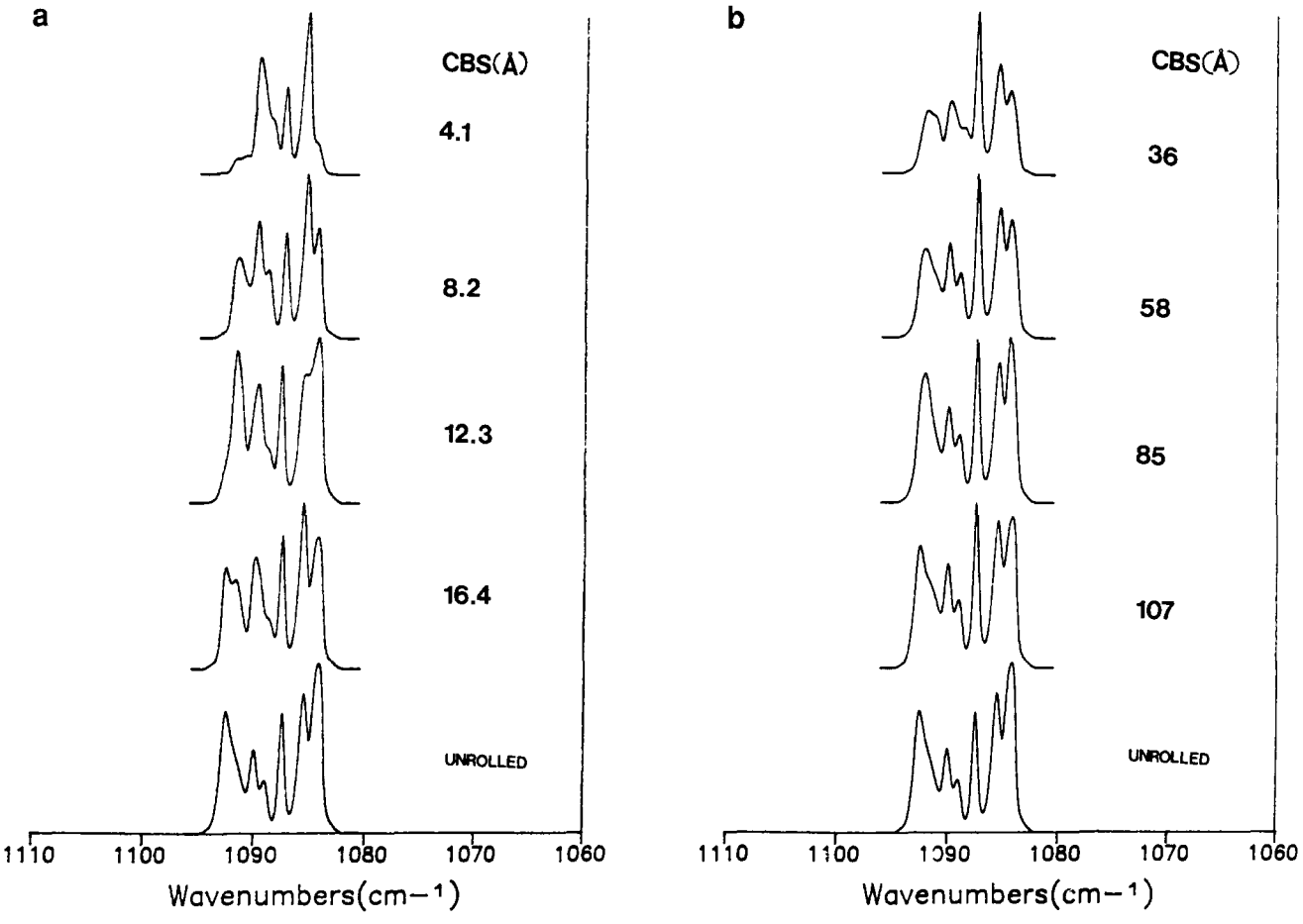

Figure 11 Calculated i.r. spectral bandshape for a seven-sheet model as a function of crystal block size (CBS) for (a) the sheet separation process and (b) for cracks parallel to the crystallographic *a*-axis. For the sheet separation process, the cracks are parallel to the [110] fold direction

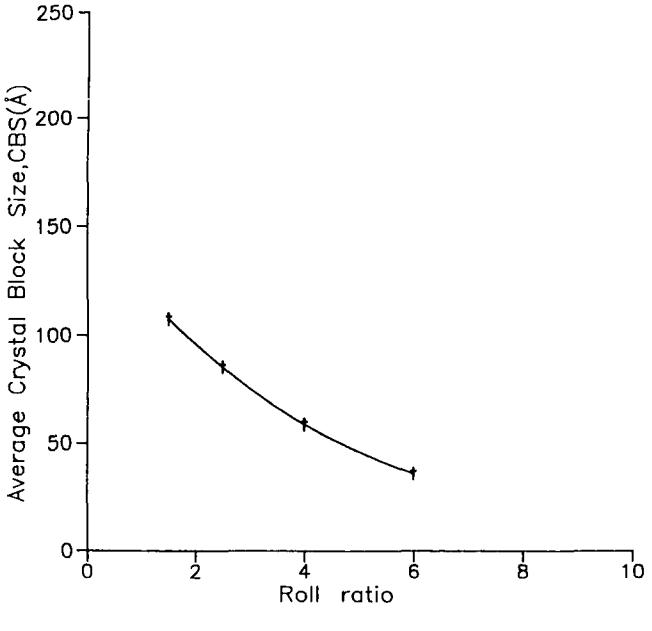

Figure 12 Variation of estimated average crystal block size with roll ratio ε

through the rotation of crystal blocks, and have shown that the stacking of these blocks becomes irregular. The progressive breakup of lamellae with increasing ε was modelled using a range of crack geometries. Of these, only the 'sheet separation' model was shown to be inconsistent with the data obtained, and it is suggested that the other processes may occur in combination. The cracks are penetrated by molecular segments pulled from adjacent crystallites (that broke away from the parent lamellae) as they separate from each other and also rotate, so as to align the molecular axis in the roll direction. The orientation, adjacency and dilution of the as-grown groups of labelled crystal stems from an individual molecule are modified and consequently the i.r. bandshape changes. A quantitative analysis of the i.r. results reveals that the average crystallite size decreases with ε, reducing to ~ 36 Å for $\varepsilon = 6$. This information is uniquely available from mixed crystal i.r. spectroscopy.

It has been assumed that cracks follow definite crystallographic directions oriented perpendicular (or nearly so) to the roll direction. Comparison of calculated data with non-polarized experimental i.r. spectra appeared to suggest that the preferential orientation of the crystallographic *b*-axis in the plane of the mat might well originate (due probably to the polyethylene single crystal domain structure) from some combination of different crack orientations during deformation.

It is necessary to consider these results in the context of previous work on the plastic deformation of polyethylene. As is the case with annealing studies, it is important to distinguish between studies on individual crystals and those relating to mats. Definitive work on single crystals drawn on substrates[18–20] has demonstrated the importance of slip, twinning and martensitic transformations. The relationship between the mode of

deformation and the crystal orientation with respect to the draw direction has indicated different behaviour in the different crystal sectors[20], implying that the crystal folds influence the process of plastic deformation. It is interesting to note that extensive slip was only observed on a plane parallel to the fold plane, a circumstance which has been shown here to produce drastic reductions in i.r. doublet splittings. Further, some of the processes envisaged by Allan and Bevis[20] would lead to a significant extension of folds which are initially compact, which would give rise to an enhanced CD_2 singlet in the i.r. spectrum. The experimentally observed twinning of lamellae on deformation to $>15\%$ is a feature which is not reproduced in our results.

Turning to previous work on single crystal mats, Ishikawa *et al.* observed that, for mats drawn above 90°C, the crystallographic *a*-axis tends to orient in the direction of drawing, at 35–40° to the mat plane, while the *b*-axis orients perpendicular to the draw direction in the mat plane[21]. A slight decrease in the long spacing was observed. Rolling annealed mats at 90°C led to approximately the same orientation of crystallographic axes for modest ε, with a four-point SAXS pattern[14]. The initial long spacing of ~ 300 Å was reduced significantly by rolling. Processes of interlamellar slippage, tilting of chains, rotation of crystallites about the *b*-axis and the *b*-axis orientation previously described were identified. Together with the disintegration into blocks, which become incorporated into microfibrils in the case of drawing, these features are the basis of Peterlin's model of plastic deformation[1,3]. A significant difference between the rolling of melt- and solution-crystallized polyethylene was found to be the absence of partial melting in single crystals, with rapid heat dissipation as the cause proposed[3]. The Peterlin model differs from Kobayashi's view of the straightening of folded chains to give bundles of extended chains, with complete unfolding in the neck[22].

A related morphology of polyethylene, obtained by casting thin films from the melt, was investigated by Petermann *et al*[4]. Electron microscopy of drawn samples led to a model of chain unfolding within a narrow deformation region. As with Kobayashi's model, blocks from the original lamellae are not preserved in the final structure.

It is clear from this discussion that the fate of blocks of crystal stems from the as-grown crystallites is a critical feature of any model. As we have shown, this information is readily available from mixed crystal measurements, and we can thus make valid comments on models such as those described above. The persistence of groups of adjacent labelled stems in samples rolled to $\varepsilon = 6.0$ indicates that folded chain blocks are retained, as in the Peterlin model[1,3]. Other features of this model are also reproduced, with the exception of chain tilt. Furthermore, the mixed crystal techniques have enabled us to estimate the lateral size of these blocks as a function of ε.

Finally, possible inadequacies in the model calculations will be considered here. The basic limitations of our models include neglecting the polydispersity of the guest molecules, the distribution of the crystallite sizes and their reorientation as a function of ε, as well as considering the separation of blocks from the original lamellae as the main feature leading to a change in the CD_2 bending spectrum. Further, specific deformation processes have been considered in turn as representative of the deformation mechanism of all polyethylene lamellae. It is evident, from previous detailed studies of the deformation of isolated single crystals, that various processes occur simultaneously. Inhomogeneity of the stress field[3] is likely to produce an inhomogeneous morphology. Our approach has been to limit the variables in our model to a manageable number. Thus, a single number of sheets has been used rather than a distribution, and stems from a single molecule have also been strictly confined to these sheets without any possibility of the occasional sequence (other than the superfolded ribbons) in another sheet. The size of the crystal blocks for each ε was determined by fitting to experimental data, without using a distribution of sizes which might include undeformed crystalline lamellae. An average orientation of the crystallites, as obtained from i.r. and WAXS, was introduced into the calculations instead of a distribution. Obviously, such factors may account for some differences between experimental and calculated data, but the general level of agreement provides confidence in the deformation processes reported and, specifically, in the variation of crystal block size.

ACKNOWLEDGEMENTS

We are grateful to the SERC for support for one of us (EUO). We would also like to thank Dr C. Booth and Mr P. J. Kobryn (University of Manchester) for the use of their Raman spectrometer and Dr P. J. Barham and Mrs A. Halter (University of Bristol) for providing PED fractions and for helpful discussions. We are grateful to Sean Dennis for i.r. measurements on the monoclinic phase.

REFERENCES

1 Peterlin, A. *J. Mater. Sci.* 1971, **6**, 490
2 Bowden, P. B. and Young, R. J. *J. Mater. Sci.* 1976, **9**, 2034
3 Peterlin, A. *Kolloid Z. Z. Polym.* 1969, **233**, 857
4 Petermann, J., Kluge, W. and Gleiter, H. *J. Polym. Sci., Polym. Phys. Edn* 1979, **17**, 1043
5 Marikhin, V. A. *Makromol. Chem. Suppl.* 1984, **7**, 147
6 Spells, S. J. and Sadler, D. M. *Polymer* 1984, **25**, 739
7 Spells, S. J., Keller, A. and Sadler, D. M. *Polymer* 1984, **25**, 749
8 Spells, S. J. and Okoroafor, E. U. *Polymer* 1994, **35**, 4590
9 Spells, S. J. *Polymer* 1985, **26**, 1921
10 Sadler, D. M. and Keller, A. *Science* 1979, **203**, 263
11 Spells, S. J. and Sadler, D. M. *Macromolecules* 1989, **22**, 3941, 3948
12 Hendra, P. J., Taylor, M. A. and Willis, H. A. *Polymer* 1985, **26**, 1501
13 Fraser, G. V. *Ind. J. Appl. Phys.* 1978, **16**, 344
14 Miyasaka, K. and Ishikawa, K. *Progr. Polym. Sci. Jpn* 1973, **6**, 153
15 Hosemann, R., Cackovic, H. and Wilke, W. *Naturwissenschaften* 1967, **11**, 278
16 Andrianova, G. P. in 'Advances in Polymer Science' (Ed. Z. A. Rogovin), Wiley, New York, 1974, p. 150
17 Barnes, J. and Fanconi, B. *J. Phys. Chem. Ref. Data* 1978, **3**, 1309
18 Kiho, H., Peterlin, A. and Geil, P. H. *J. Appl. Phys.* 1964, **35**, 1599
19 Geil, P. H., Kiho, H. and Peterlin, A. *J. Polym. Sci.* 1964, **B2**, 71
20 Allan, P. and Bevis, M. *Proc. R. Soc. (London) A* 1974, **341**, 75
21 Ishikawa, K., Miyasaka, K. and Maeda, M. *J. Polym. Sci. A2* 1969, **7**, 2029
22 Peterlin, A. *J. Polym. Sci. C* 1965, **9**, 61